Available online at www.sciencedirect.com

ScienceDirect

Energy Procedia 61 (2014) 1402 – 1409

Energy Procedia

The 6th International Conference on Applied Energy – ICAE2014

Comparison electrochemical performances of spherical $LiFePO_4$/C cathode materials at low and high temperatures

*,[2]Chun-Chen Yang, [1,2]Jer-Huan Jang, [1,2]Jia-Rong Jiang

*Department of Chemical Engineering, Ming Chi University of Technology, New Taipei City 243, Taiwan, R.O.C.
[1]Department of Mechanical Engineering, Ming Chi University of Technology, New Taipei City 243, Taiwan, R.O.C.
[2]Battery Research Center of Green Energy, Ming Chi University of Technology, New Taipei City 243, Taiwan, R.O.C.

Abstract

The spherical $LiFePO_4$/C composite material was prepared by the solid-state method and a spray dry method. The surface modification was conducted on spherical LFP/C composite by using 3wt.% $Li_4Ti_5O_{12}$ (LTO) to improve the rate capability and cycle stability properties at a low temperature of -20°C and a high temperature of 55°C. The characteristic properties were examined by X-ray diffraction (XRD), micro-Raman, scanning electron microscopy (SEM), AC impedance method, and galvanostatic charge-discharge method. For comparison, the as-prepared $LiFePO_4$/C cathode, SP LFP/C composite, and 3%LTO-modified spherical $LiFePO_4$/C composite are studied and compared. As a result, the LTO-modified spherical $LiFePO_4$/C composite displays the discharge capacities of 150, 145, 135, 110, 95 and 90 mAh g^{-1} at 0.1C, 0.2C, 0.5C, 1C, 3C and 5C rates, respectively. It is demonstrated that the LTO-modified spherical $LiFePO_4$/C composite material exhibit a good candidate for application in Li ion batteries.

Peer-review under responsibility of the Organizing Committee of ICAE2014

Keywords: Spray dry, $LiFePO_4$, $Li_4Ti_5O_{12}$ (LTO), surface modified, Li ion batteries

1. Introduction

Lithium-ion batteries, due to their relatively high specific capacity, are considered for electric vehicle (EV), cell phones, laptop computers, digital cameras, renewable energy storage, and smart grid applications. The $LiFePO_4$ cathode material proposed by Padhi et al. [1] has attracted extensive attention for application in the next generation of rechargeable lithium-ion batteries due to its low cost, environmental benignancy, excellent safety characteristics, high capacity (theoretical capacity ~170 mAh g^{-1}), and excellent cycling performance. However, its poor conductivity, for electron and ion transfer, is the major barriers for commercial applications. The electron conductivity of $LiFePO_4$ is only 10^{-9} S cm^{-1} [2] and its lithium ion diffusivity is 10^{-14} ~ 10^{-16} cm^2 s^{-1} [3]. There are three methods to improve the electronic conductivity, which include the following: (1) carbon coating; (2) doping with supervalent cations; (3) decrease the particle size. The carbon coating is the most effective among these methods, and is a facile way to improve the conductivity of $LiFePO_4$ materials. The $LiFePO_4$ cathode materials can usually be prepared via a solid-state reaction [4,5], sol-gel process [6,7], and hydrothermal process [8-13]. Whittingham [8] revealed that the high-quality crystalline $LiFePO_4$ platelets can be obtained by a low temperature hydrothermal process. Spray dry (SP) method was widely used to prepare spherical $LiFePO_4$/C cathode material to enhance the electrochemical performance [14-18]. The low and high temperature performance and capacity fading mechanism of $LiFePO_4$/C material have been pay great attention recently [19-24]. The surface modification of LiFePO4/C became an important issue for improve the low and high temperature electrochemical properties [**25-28**].

* Corresponding author. Tel.: +886-2-2908-9899; fax: +886-2-2908-5941.
E-mail address: ccyang@mail.mcut.edu.tw

Peer-review under responsibility of the Organizing Committee of ICAE2014
doi:10.1016/j.egypro.2014.12.136

In this work, we first prepared the $LiFePO_4$/C (denoted as LFP/C) composite materials by a solid-state method. The spray dry method and post-sintering were used to prepare spherical LFP/C composite. A suitable amount of glucose was added as the binder and the carbon source during the spray dry processing. In order to improve the low and high temperature performance of LFP/C material, the $Li_4Ti_5O_{12}$ (LTO) surface modification was applied to SP LFP/C composite by a sol-gel method. For comparison, we also prepared the $LiFePO_4$/C material without PSS template. The characteristic properties of $LiFePO_4$/C composite material with and without polymer template were examined by X-ray diffraction (XRD), micro-Raman spectroscopy, scanning electron microscopy (SEM), elemental analysis (EA), and Micro-Raman spectroscopy. The electrochemical performances of the Li/$LiFePO_4$ coin cell were examined by an automatic galvanostatic charge/discharge unit and a cyclic voltammetry method.

2. Experimental

2.1 Preparation of $LiFePO_4$/C composite materials

The $LiFePO_4$/C materials were prepared by a solid state method. The appropriate quantities of LiH_2PO_4, $FeC_2O_4.2H_2O$, 5%sucrose, and 5% citric acid (Aldrich) as the starting materials were all mixed in acetone and then ball-milled at a rotation speed of 400 rpm for 6 h in a planetary miller with a ball/reactant weight ratio of 6:1. The added carbon source in the $LiFePO_4$/C materials was maintained at 10wt.%. The ball-milled mixture precursor was pre-sintered at 350°C for 4 h and then sintered at 700°C for 12 h under an Ar/H_2 (95:5, v/v) atmosphere.

The spherical $LiFePO_4$/C composite materials were prepared by a spray dry method and a post-sintering process. The appropriate quantities of $LiFePO_4$/C materials and 5% glucose were dissolved in deionized water. The spherical LFP/C composite with a double carbon source was prepared a spray dryer (EYELA, Spray Dryer SD-1000 model, Japan). The obtained spherical LFP/C composite powder was further calcined at 700°C for 5 h in an Ar atmosphere.

The LTO-coated spherical LFP/C materials were synthesized by a sol-gel method. $Ti(C_4H_9O)_4$ and $CH_3COOLi.2H_2O$ with a Li:Ti stoichiometric amount of 4:5 molar ratio were dissolved in a solution contained ethanol and distilled water fo form a clear solution. Then, a small amount of HNO_3 was added into the above solution with a continuous stirring to obtain a sol. The SP-LFP/C composite powder was slowly added to the above sol under stirring. After hydrolyzing and condensation for 10h, a black gel was formed. Finally, the obtained gel was dried at 120°C for 2h and then calcined at 700°C for 3h to obtained the final surface-modified spherical LFP/C composite powders.

2.2 Characterization

The crystal structure of all LFP/C composite samples was examined by an X-ray diffraction (XRD) spectrometer (Philip, X'pert Pro System). The surface morphology was conducted by a scanning electron microscope (SEM, Hitachi). The Micro-Raman spectra were recorded on a confocal micro-Renishaw with a 632 nm He-Ne laser excitation. The residual carbon content in the sample was analyzed using Elemental Analyzer (Perkin Elmer 2400). The electron conductivity of the composite samples was measured by AC impedance method.

2.3 Electrochemical measurements

The electrochemical performances of the Li/$LiFePO_4$ composite battery were measured by using a two-electrode system (CR 2032 coin cell assembled in an argon-filled glove box). All $LiFePO_4$/C composite electrodes were prepared by mixing active $LiFePO_4$/C materials, Super P, and poly(vinyl fluoride) (PVDF) binder in a weight ratio of 90:5:5, pasted on an aluminum foil (Aldrich), and then dried in a vacuum oven at 120°C for 12 h. The lithium foil (Aldrich) was used as the counter and reference electrode. A micro-porous PE film was used as the separator. The electrolyte was 1 M $LiPF_6$ in a mixture of EC and DEC (1:1 in v/v, Merck). The $LiFePO_4$/Li composite batteries were charged by a constant current profile (CC) and discharged by a constant current profile, over a potential range of 2.0 - 3.8 V (vs. Li/Li^+) at varied C rates with an Autolab PGSTAT302N potentiostat. The cyclic voltammetry (CV) was conducted by using an Autolab instrument at a scanning rate of 0.1 mV s^{-1} between 2.5 and 4.2 V.

3. Results and discussion

The XRD patterns of LFP/C materials with or without a polymer template prepared by the solid state method are shown in Fig. 1, respectively. The XRD diffraction patterns revealed that the as-prepared LFP/C, SP-LFP/C composite, and 3%LTO modified SP-LFP/C composite are all single phase materials with an olivine-type structure indexed to the orthorhombic *Pnma* space group. The diffraction peak of the residual carbon can not be found in the pattern; and may be their low content or amorphous state. The lattice parameters (a, b, c, and cell volume) of the as-prepared $LiFePO_4$/C sample with spray dry and 3%LTO surface modified SP-LFP/C samples were

calculated based on the XRD patterns. It was found that the lattice parameters of all LFP/C samples are the same as the standard $LiFePO_4$ (JCPDS card number 81-1173, a=10.33Å, b= 6.010 Å, c=4.692 Å, V =291.35 (Å)^3). The LTO and carbon source of glucose and citric acid have no observable influence on the structure of LFP/C composite materials. There is no impurity phase occurred.

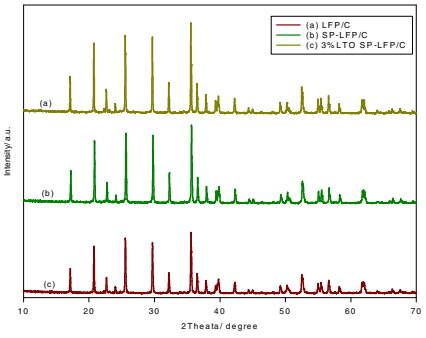

Fig. 1 XRD patterns of LFP/C, SP- LFP/C, SP 3%LTO-LFP/C samples.

The SEM image of the LFP/C material prepared by the solid state method is shown in Fig. 2(a). Generally, the particle size increased when the sintering temperature was increased. The particle size of the LFP/C sample is in the range of 0.5 - 2 µm. Consequently, the addition of citric acid and sucrose as the carbon source not only decreased particle size but also prevented the particle from growing during the sintering process.

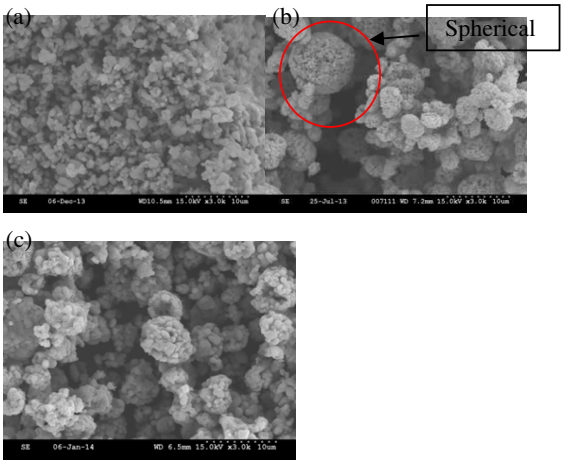

Fig. 2 SEM images of (a). LFP/C sample; (b). SP LFP/C, and (b). SP LTO-LFP/C samples

The SEM image of SP-LFP/C composite prepared by a spray dry method sintered at 700°C is shown in Fig. 2(b). The particle size of the SP-LFP/C composite sample is in the range of 2 - 10 µm. It was found that there are many micro-pores formed on surface of SP-LFP/C material, and it acts as a micro-reservoir for electrolyte. The highly porous and spherical morphology for SP-LFP/C composite can markedly enhance the mass transport properties. Fig. 2(c) shows the SEM image of 3%LTO modified SP-LFP/C composite prepared by a sol-gel method. The particle size of 3%LTO modified SP-LFP/C composite is in the range of 2 - 8 µm. It was found that there are also many micro-pores formed on surface of 3%LTO modified SP-LFP/C material and it acts as a micro-reservoir for electrolyte. The highly porous and spherical morphology for SP-LFP/C composite can substantially improve the electrochemical properties.

of the $LiFePO_4$/C sample is in the range of 1 - 5 µm. Consequently, the addition of citric acid and sucrose as the carbon source not only decreased particle size but also prevented the particle from growing during the sintering process. The SEM image of 1%Nb doped $LiFePO_4$/C composite + 10%PSS template prepared by the solid state method at 700°C is shown in Fig. 2(b). The particle size of the $LiFePO_4$/C +10%PSS template is in the range of 0.5 - 2 µm. It was found that there are many micro-pores (about 100 nm) formed on surface of LFP/C material, and it acts as a micro-reservoir for electrolyte. Those micropores can markedly enhance the mass transport properties of LFP/C composite materials. The $LiFePO_4$/C particle size increased when the sintering temperature was varied in the range of 600-700°C. It was found that the optimum sintering temperature is around 700 °C in this work.

In addition, Micro-Raman spectra of the LFP/C, SP-LFP/C, and 3%LTO modified SP-LFP/C samples prepared by a solid state method and a spray dry method, respectively, are show in Fig. 3. The Raman peaks of $LiFePO_4$/C material located at approximately 1328 and 1590 cm^{-1} can be identified as arising from citric acid and sucrose carbon source. The Raman peaks at approximately 1328 cm^{-1} (D band) and 1590 cm^{-1} (G band) are observed in the composite samples. The Raman peaks of SP-LFP/C samples located at approximately 1332 and 1590 cm^{-1} are identified as arising from the residual carbon of glucose and citric acid. The Raman peaks at approximately 1330 cm^{-1} (D band) and 1586 cm^{-1} (G band) are also observed in the 3%LTO modified SP-LFP/C composite samples. The broadening of the D (A_{1g} symmetry) band and G (E_{2g} symmetry) band with a strong D band indicates a localized in-plane sp^2 graphitic crystal domain and a disordered sp^3 amorphous carbon. The intensity ratio of the D band vs. the G band (denoted as $R=I_D/I_G$) can be used to

estimate the carbon quality of the $LiFePO_4$/C samples. It was found that the *R* value of the 3%LTO modified SP-LFP/C and SP-LFP/C composite sample are around 1.02-1.10. By comparison, the *R* value of $LiFePO_4$/C samples without template around 1.45. It was reported [11] that the discharge capacity and the rate capability of the $LiFePO_4$/C samples are closely related to the intensity ratio of the D band and the G band. A number of Raman peaks located at approximately the range of 947-950 cm^{-1} and 596-446 cm^{-1} are identified as the vibration of the P-O bond and the peak located at 638 cm^{-1} is identified as the vibration of the FeO_x groups.

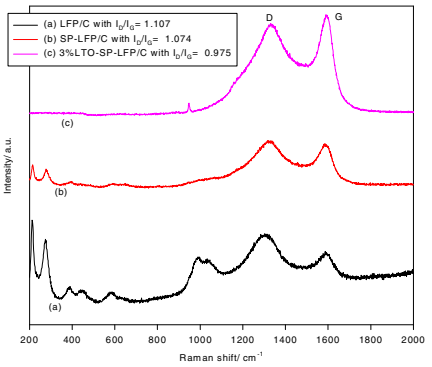

Fig. 3 Micro-Raman spectra of LFP/C sample and SP-LFP/C samples.

The electrochemical properties of $LiFePO_4$/C samples are strongly related with the electronic conductivity, the total residual carbon content, and the value of I_D/I_G ratio. Both the electronic conductivity and the total residual carbon content are significantly affected the discharge capacity and the rate capability of the LFP/C composite cathodes. The electronic conductivities (σ_e) and the residual carbon (C%) content of all $LiFePO_4$/C samples are approximately $1.10\sim3.67\times10^{-4}$ S cm^{-1} and 3.10-4.2%, respectively. These values are consistent with the reported data in the literature [1,2]. By contrast, the electronic conductivity of 3%LTO modified LFP/C composite is much higher than those of LFP/C and SP-LFP/C.

The cyclic voltammetries of the LFP/C material and spherical SP-LFP/C composite in the first cycle at a scan rate of 0.1 mV s^{-1} are shown in Fig. 4. The oxidation and reduction peaks of the LFP/C sample approximately 3.63 and 3.25 V, respectively, and the potential difference between the two peaks is 0.40 V. Furthermore, the oxidation and reduction peaks of the SP-LFP/C composite by a spray dry method at approximately 3.52 and 3.34 V, respectively, and the potential difference between two peaks is 0.180 V. However, the intensities of oxidation and reduction peak currents of SP-LFP/C composite are much higher than those of LFP/C sample. The redox peak profiles of two samples are very different. In short, the reversibility and electrochemical activity of the SP-LFP/C composite is superior to that of the LFP/C sample.

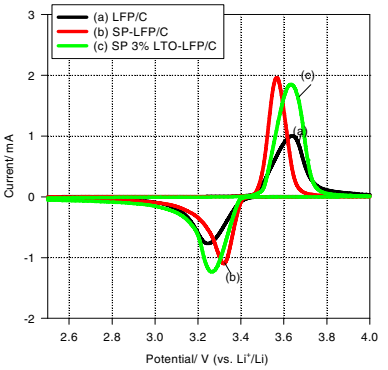

Fig. 4 The CV curves of LFP/C sample and SP-LFP/C samples at 0.1 mV s^{-1}.

Fig. 5 shows the initial charge-discharge profiles of LFP/C, SP-LFP/C, and 3%LTO modified SP-LFP/C composite samples sintered at 700°C at 0.1C rate. As shown in Fig. 5, all $LiFePO_4$/C material and SP-LFP/C and LTO-modified LFP/C composites show the flat discharge plateau at 3.40 vs. Li/Li^+. The LFP/C, SP-LFP/C, and 3%LTO modified LFP/C composite deliver the specific capacities of 133, 151 and 152 mAh g^{-1} at 0.1 C rate, respectively. It is clearly that the discharge capacity performance of the 3%LTO modified SP-LFP/C composite is superior to that of LFP/C material; however, the electrochemical performance of SP-LFP/C and 3%LTO modified SP-LFP/C is the same. It may be due to the synergistic effect of spherical morphology and surface modification.

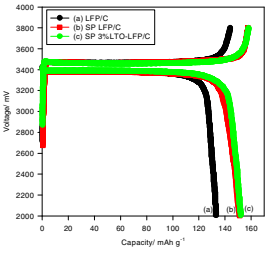

Fig. 5 The initial charge/discharge curves of LFP/C and SP-LFP/C samples at 0.1C rate.

The typical charge/discharge profiles of LFP/C, SP-LFP/C, and 3%LTO modified SP-LFP/C composite samples at 25ºC at varied rates of 0.2 to 10C are displayed in Fig.6. All $LiFePO_4$/Li half cells reveal the typical flat potential plateau at 3.3 - 3.4 vs. Li/Li^+ at 0.2-0.5C rate. The potential plateau becomes sloping when the discharge rate is higher than 1C rate. The SP-LFP/C composite delivers the specific capacities of 135, 131, 122, 103, 94, and 78 mAh g^{-1} at rates of 0.2, 0.5, 1, 3, 5, and 10C, respectively. In contrast, the 3%LTO modified SP-LFP/C composite delivers the specific capacities of 150, 141, 131, 110, 103, and 84 mAh g^{-1} at rates of 0.2, 0.5, 1, 3, 5, and 10C, respectively. However, the LFP/C sample without surface modification and non-spherical morphology delivers the specific capacities of 125, 116, 105, 87, 76, and 48 mAh g^{-1} at 0.1, 0.2, 0.5, 1, 3, 5 and 10C rates, respectively. Fig. 7 shows the comparison of the rate capability of LFP/C, SP-LFP/C, and 3%LTO coated SP-LFP/C composite at various rates. It was demonstrated clearly that both 3D porous spherical morphology and LTO surface modification (ca. 3wt.%) on LFP/C material can greatly improve the high rate capability. The dissolution of Fe^{2+} from LFP/C is one of the main reasons for capacity fading mechanism [19-24] during high temperature cycling. It was well-known that the HF generated from $LiPF_6$ electrolyte was responsible for the dissolution of Fe during cycling. The un-coated LFP/C cathode material in $LiPF_6$ electrolyte will react with HF and thus leads to a gradually capacity loss. The LTO surface coating can prevent Fe^{2+} ions from direct contacting with electrolyte and greatly decreasing the capacity loss [24,25].

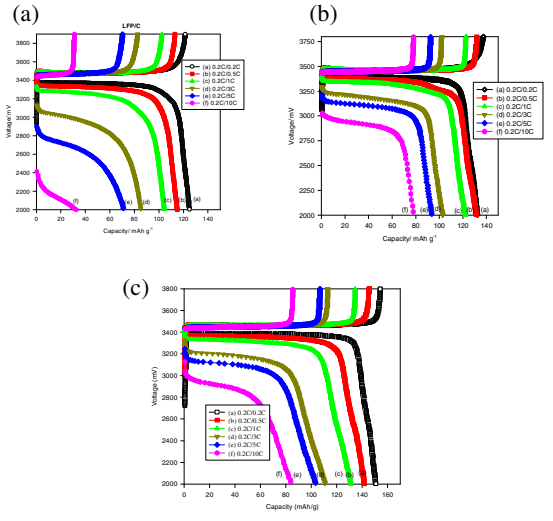

Fig. 6 The charge-discharge curve of (a). LFP, (b). SP-LFP, (c). 3%LTO-SP LFP/C samples at varied rates

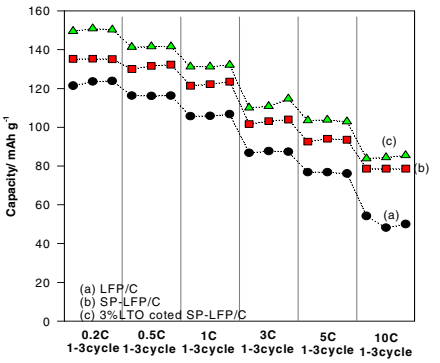

Fig. 7 The rate capability of LFP/C and SP-LFP/C samples at 0.2C to 10C rates.

Moreover, it was found that the discharge capacity and coulomb efficiency of 3%LTO SP-LFP/C composite at 1C/3C rate during 200 cycling test at 25ºC are around 100 mAh g^{-1} and 93-97%, respectively, as shown in Fig. 8. It was found that the fading rate of 3%LTO SP-LFP/C composite is around 0.01 mAh $cycle^{-1}$ at 25ºC. However, that the discharge capacity of 3%LTO SP-LFP/C composite at 1C/3C rate during 200 cycling test at 55ºC declined from 148 to 67 mAh g^{-1} with a fading rate of 0.405 mAh $cycle^{-1}$. Moreover, it was found that the discharge capacity and coulomb efficiency of 3%LTO SP-LFP/C composite at 1C/3C rate during 200 cycling test at 0ºC are around 40-42 mAh g^{-1} and 95-97%, respectively. It was found that the fading rate of 3%LTO SP-LFP/C composite is around 0.04 mAh $cycle^{-1}$ at 0ºC. It was clearly that 3%LTO SP-LFP/C composite at 55ºC (0.405 mAh $cycle^{-1}$) shows the highest fading rate, as compared with those of LTO coated LFP/C composite at 25ºC (0.01 mAh $cycle^{-1}$) and 0ºC (0.04 mAh $cycle^{-1}$). By comparison, it was found that the discharge capacity and coulomb efficiency of LFP/C without LTO coating at 1C/3C rate during 200 cycling test at 25ºC declined from 70 to 37 mAh g^{-1} with a fading rate of 0.170 mAh $cycle^{-1}$. The LFP/C sample indeed shows poor high rate capability at 3C discharge rate. It also revealed that the fading rate of LFP/C without surface modification is much higher than that of 3%LTO coated SP-LFP/C sample at 25ºC.

The AC impedance spectroscopy is used to study the interface properties of LFP/C sample and 3%LTO SP-LFP/C composite samples. The AC spectra of the 3%LTO SP-LFP/C composite sample at a temperature of 25, 0, -10, and -20ºC at open circuit potential are shown in Fig. 9(a). Each AC plot consisted of one semicircle at higher frequency followed by a linear portion at lower frequency. The lower frequency region of the straight line is considered as Warburg

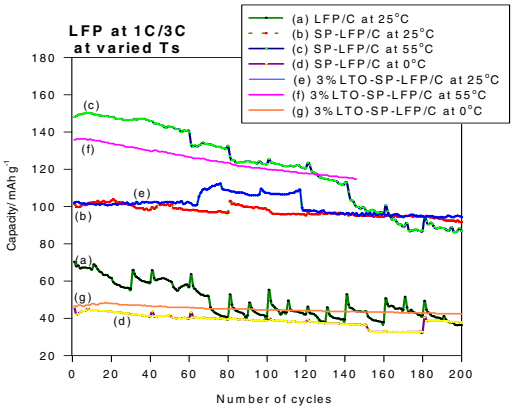

Fig. 8 The cycling and CE performance for LFP/C and SP-LFP/C samples at 1C/3C rate at 25 and 55°C.

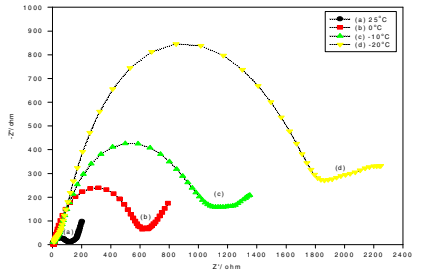

(a)

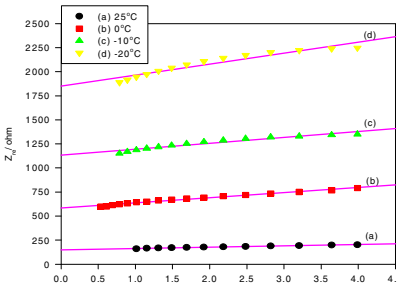

(b)

Fig. 10 The AC impedance spectra for 3%LTO SP-LFP/C composite (a) and (b); Z' vs. $w^{-1/2}$ curve for 3%LTO coated SP-LFP/C composite.

impedance. It is for long-range lithium ion diffusion in bulk phase. The R_b indicates the bulk resistance at the electrolyte; R_{ct} is attributed to the charge transfer resistance at the active material interface; CPE represents the double layer capacitance and some surface film capacitance. The lithium chemical diffusion coefficients (D_i) of the electrode were calculated based on the equation (1) [19-24]:

$$D_i = \frac{1}{2}\left(\frac{RT}{AF^2\sigma C}\right)^2 \quad (1)$$

Where σ is Wargurg impedance coefficient (obtained a slope from plot of Z_{re} vs.$\varpi^{-0.5}$, as seen in Fig. 9(b); D_i is the lithium diffusion coefficient; R is the gas constant; T is the absolute temperature; F is Faraday's constant; A is the area of the electrode; C is the molar concentration of Li^+ ions (C_{Li+}=1.0×10^{-3} mol cm^{-3}). **Tables 1 and 2** show the calculated R_b, R_{ct}, D_i, j_o parameters for LFP/C material and 3%LTO SP-LFP/C composite sample. It was found that the R_b values of LFP/C material sample at the temperature of 25, 0, -10, and -20°C are 5.14, 7.25, 9.11, 12.19 ohm, respectively. The lower temperature is the test, the higher is the value of R_b. It is due to the lower the ionic conductivity of the electrolyte. The values of R_{ct} and D_i for LFP/C samples are greatly varied. It was found that the R_{ct} values of LFP/C material sample at the temperature of 25, 0, -10, and -20°C are 123.5, 615.0, 1133, 1862 ohm, respectively. It was found that the D_i values of LFP/C material sample at the temperature of 25, 0, -10, and -20°C are 2.61×10^{-14}, 3.00×10^{-15}, 9.71×10^{-15}, 3.65×10^{-16} cm^2 s^{-1}, respectively.

Table 1. Impedance parameters derived using equivalent circuit model and lithium diffusion coefficient D for Irregular form $LiFePO_4$/C electrode (100% DOD)

Param. / Temp/ °C	R_b (Ω)	R_{ct} (Ω)	D (cm^2/s)
25	5.14	123.5	2.61×10^{-14}
0	7.25	615.0	3.00×10^{-15}
-10	9.11	1133.0	9.71×10^{-16}
-20	12.19	1862.0	3.65×10^{-16}

Table 2
Impedance parameters derived using equivalent circuit model and lithium diffusion coefficient D for SP-$LiFePO_4$/C powders cathode (100%DOD).

Param. / Temp/ °C	R_b (Ω)	R_{ct} (Ω)	D (cm^2/s)
25	5.67	135.2	1.80×10^{-12}
0	8.19	195.7	1.00×10^{-13}
-10	8.85	315.4	7.00×10^{-14}
-20	11.43	622.1	1.88×10^{-14}

Accordingly, It was found that the R_b values of 3%LTO SP-LFP/C composite sample at the temperature of 25, 0, -10, and -20ºC are 5.67, 8.19, 8.85, 11.43 ohm, respectively. The lower temperature is the test, the higher is the value of R_b. It is due to the lower the ionic conductivity of the electrolyte. The values of R_{ct} and D_i for composite samples are greatly varied. It was found that the R_{ct} values of 3%LTO SP-LFP/C composite at the temperature of 25, 0, -10, and -20ºC are 135.2, 195.7, 315.4, 622.1 ohm, respectively. It was found that the D_i values of LFP/C material sample at the temperature of 25, 0, -10, and -20ºC are 1.80×10^{-12}, 1.00×10^{-13}, 7.00×10^{-14}, 1.88×10^{-14} cm^2 s^{-1}, respectively. It demonstrates that the low temperature performance of LFP/C with spherical morphology and LTO surface modification is much better that that of irregular morphology LFP/C without surface modification. The R_{ct} and D_i values of 3%LTO SP-LFP/C composite are much higher than those of LFP/C material. It is due to the transport properties improvement, in particular, for R_{ct} and D_i. As a result, through spray dry spherical morphology and the surface modification on LFP/C cathode material can greatly improve the electrochemical performance and rate capability at lower temperature.

Figs. 10(a) and (b) shows the Arrhenius plot based on R_b and R_{ct} values at different test temperatures, i.e., 25, 0, -10, and -20ºC. According to the plot, the activation energy values of LFP/C material and 3%LTO SP-LFP/C composite can be obtained. It was found that the activation energy values ($E_{a,Rb}$) of LFP/C and 3%LTO SP-LFP/C composite based on R_b are 13.19 and 10.40 kJ mol^{-1}, respectively. This $E_{a,Rb}$ value is closely related to the current collector, active material conductivity. It seems about the magnitude order for two as-prepared LFP materials. However, the activation energy values ($E_{a,Rct}$) of LFP/C and 3%LTO SP-LFP/C composite based on R_{ct} are 42.12 and 23.07 kJ mol^{-1}, respectively. This $E_{a,Rct}$ value is closely related to the charge transfer at the interface of electrode and electrolyte. The high $E_{a,Rct}$ value of LFP/C material (42.12 kJ mol^{-1}) indicates poor electrochemical performance, as compared with that of 3%LTO SP-LFP/C composite (23.07 kJ mol^{-1}).

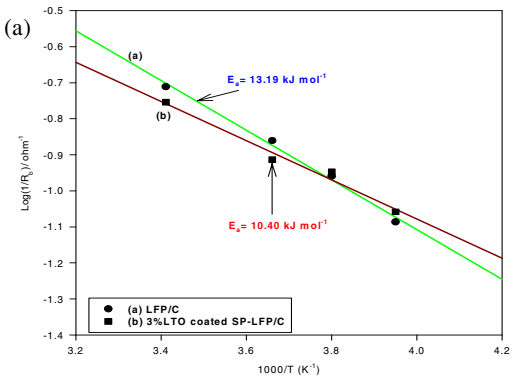

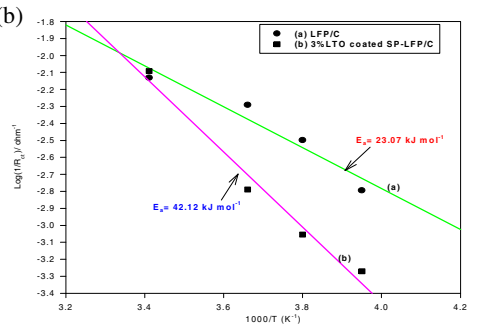

Fig. 10 The Arrhenius plot for(a) LFP/C and (b)3%LTO coated SP-LFP/C composite.

4. Conclusions

The spherical LFP/C composite was prepared by the solid-state method and a spray dry method. The surface modification was conducted on spherical LFP/C composite by using 3wt.% $Li_4Ti_5O_{12}$ (LTO) to improve the rate capability and cycle stability properties at a low temperature of -20ºC and a high temperature of 55ºC. The characteristic properties were examined by X-ray diffraction (XRD), micro-Raman, scanning electron microscopy (SEM), AC impedance method, and galvanostatic charge-discharge method. For comparison, the as-prepared $LiFePO_4$/C cathode, SP LFP/C composite, and 3%LTO-modified spherical $LiFePO_4$/C composite are studied and compared. As a result, the 3%LTO modified spherical $LiFePO_4$/C composite displays the discharge capacities of 150, 141, 131, 110, 103 and 84 mAh g^{-1} at 0.2C, 0.5C, 1C, 3C, 5C and 10C rates, respectively.

It also showed that 3%LTO SP-LFP/C composite at 55ºC (0.405 mAh $cycle^{-1}$) exhibits the highest fading rate, as compared with those of 3%LTO coated SP-LFP/C composite at 25ºC (0.01 mAh $cycle^{-1}$) and 0ºC (0.04 mAh $cycle^{-1}$). Moreover, it was found that the discharge capacity and coulomb efficiency of LFP/C without LTO coating at 1C/3C rate during 200 cycling test at 25ºC declined from 70 to 37 mAh g^{-1} with a fading rate of 0.170 mAh $cycle^{-1}$. The LFP/C sample indeed shows poor high rate capability at 3C discharge rate. It also revealed that the fading rate of LFP/C without surface modification is much higher than that of 3%LTO coated SP-LFP/C sample at 25ºC. It is demonstrated that the LTO-modified spherical $LiFePO_4$/C composite material exhibit a good candidate for application in Li ion batteries at lower and high temperature applications.

5. Acknowledgements

Financial support from the National Science Council, Taiwan (Project No: NSC 102-2632-E-131-001-MY3) is gratefully acknowledged.

6. References

[1] A.K. Padhi, K.S. Nanjundaswamy, J.B. Goodenough, J. Electrochem. Soc. 144 (1997) 1188-1194.
[2] S.Y. Chung, Y.M. Chiang, Electrochem. Solid State Lett. 6 (2003) A278-A281.
[3] P.P. Prosini, M. Lisi, D. Zane, M. Pasquali, Electrochem. Solid-State Ionics 148 (2002) 45-51.
[4] N. Meethong, H.-Y. Huang, S.A. Speakman, W.C. Carter, Y.-M. Chiang Adv. Funct. Mater. 17 (2007) 1115-1123.
[5] A. Yamada, S.C. Chung, K. Hinokuma, J. Electrochem. Soc. 148 (2001) A224-A229.
[6] J. Yang, J.J. Xu, Electrochem. Solid-State Lett. 7 (2004) A515-A518.
[7] C.R. Sides, F. Croce, V.Y. Young, C.R. Martin, B. Scrosatia, Solid-State Lett. 8 (2005) A484-A487.
[8] S. Yang, P.Y. Zavalij, M.S. Whittingham, Electrochem. Commun. 5 (2001) 505-509.
[9] J. Chen, M.S. Whittingham, Electrochem. Commun. 5 (2006) 855-858.
[9] J. Chen, S. Wang, M.S. Whittingham, MS, J. Power Sources 174 (2007) 442-448.
[10] J. Chen, M.J. Vacchio, S. Wang, N. Chernova, P.Y. Zavalij, M.S. Whittingham, Solid State Ionics 178 (2008)1676-1693.
[11] M.M. Doeff, Y. Hu, F. McLarnon, R. Kostecki, (2003) Electrochem. Solid-State Lett 6 (2003) A207-A222.
[12] X. Huang, S. Yan, H. Zhao, L. Zhang, R. Guo, C. Chang, X. Kong, H. Han, Mater. Charact. 61 (2010) 720-725.
[13] F. Teng, S. Santhanagopalan, R. Lemmens, X. Geng, P. Patel, Solid State Science 12 (2010) 952-955.
[14] F. Gao, Z. Tang, J. Xue, Electrochim. Acta 60 (2012) 269-273.
[15] L. Wu, S.-K. Zhong, J.-Q. Liu, F. Lv, K. Wan, Mater. Lett. 89 (2012) 32-35.
[16] M. Konarova, I. Taniguchi, Powder Technol. 191 (2009) 111-116.
[17] M. Konarova, I. Taniguchi, J. Power Sources 195 (2010) 3661-3667.
[18] S. Zhong, L. Wu, J. Zheng, J. Liu, Powder Technol. 219 (2012) 45-48.
[19] X. Liao, Z. Ma, Q. Gong, Y. He, Li Pei, L. Zeng, Electrochem. Commun. 10 (2008) 691-694.
[20] K. Yang, Z. Deng, J. Suo, J. Power Sources 201 (2012) 274-279.
[21] L. Liao, P. Zuo, Y. Ma, X. Chen, Y. An, Y. Gao, G. Yin, Electrochim. Acta 60 (2012) 269-273.
[22] Y. Zhang, C. Wang, X. Tang, J. Power Sources 196 (2011) 1513-1520.
[23] H. Song, Z. Cao, X. Chen, H. Lu, M. Jia, Z. Zhang, Y. Lai, J. Li, Y. Liu, J. Solid State Electrochem. 17 (2013) 599-605.
[24] J. Kim, S. Woo, M. Park, K. Kim, T. Yim, J. Kim, Y. Kim, J. Power Sources 229 (2013) 190-197.